Nucleation-Elongation Dynamics of Two-Dimensional Covalent Organic Frameworks

Haoyuan Li[a§], *Austin M. Evans*[b§], *Ioannina Castano*[b], *Michael J. Strauss*[b], *William R. Dichtel*[b]* *and Jean-Luc Bredas*[a]*

[a]School of Chemistry and Biochemistry, Center for Organic Photonics and Electronics (COPE), Georgia Institute of Technology, Atlanta, Georgia 30332-0400

[b]Department of Chemistry, Northwestern University, Evanston, IL 60208, USA.

[§]These authors contributed equally to this work.

Corresponding Authors

*jean-luc.bredas@chemistry.gatech.edu

*wdichtel@northwestern.edu

ABSTRACT

Homogeneous two-dimensional (2D) polymerization is a poorly understood process in which topologically planar monomers react to form planar macromolecules, often termed 2D covalent organic frameworks (COFs). While these COFs have traditionally been limited to weakly crystalline aggregated powders, they were recently grown as micron-sized single crystals by temporally resolving the growth and nucleation processes. Here, we present a quantitative analysis of the nucleation and growth rates of 2D COFs via kinetic Monte Carlo (KMC) simulations, which show that nucleation and growth have second-order and first-order dependences on monomer concentration, respectively. The computational results were confirmed experimentally by systematic measurements of COF nucleation and growth rates performed via *in situ* X-ray scattering, which validated the respective monomer concentration dependences of the nucleation and elongation processes. A major consequence is that there exists a threshold monomer concentration below which growth dominates over nucleation. Our computational and experimental findings rationalize recent empirical observations that, in the formation of 2D COF single crystals, growth dominates over nucleation when monomers are added slowly, so as to limit their steady-state concentration. This mechanistic understanding of the nucleation and growth processes will inform the rational control of polymerization in two dimensions and ultimately enable access to high-quality samples of designed two-dimensional polymers.

TOC GRAPHICS

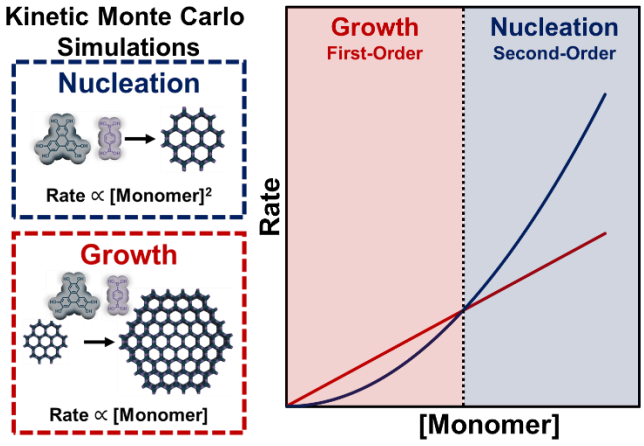

KEYWORDS: Covalent organic frameworks (COFs); two-dimensional (2D) materials; kinetic Monte Carlo simulations; two-dimensional polymer networks; *in situ* X-ray diffraction

Introduction

Two-dimensional (2D) polymerization is an emerging frontier in polymer science, which promises the development of rationally designed 2D materials.[1] 2D covalent organic frameworks (COFs) are a class of 2D polymers that are permanently porous, atomically regular, synthetically modular, and structurally versatile.[2-14] These properties have inspired explorations of COFs for applications such as catalysis, molecular separations, energy storage, and optoelectronic devices.[15-34] However, their small crystalline domain sizes (< 100 nm) and empirical polymerization processes have impeded the study of their intrinsic properties. It has been suggested that the insufficient materials quality of the 2D COFs obtained to-date is likely due to uncontrolled nucleation-elongation processes in the reaction mixture.[35-38] However, characterizing the small, polydisperse, constantly evolving particles present in the early stages of COF polymerization remains a demanding experimental task. From a theoretical perspective, using an analytical approach to describe the nucleation and growth rates is also daunting because of the presence of many simultaneous growth processes and pathways.[39] Furthermore, the application of computational methods such as molecular dynamics (MD) simulations provides only limited information because of the short time scales that are accessible.[40]

Recently, Smith *et al.* demonstrated a novel synthetic method that prevents agglomeration of COF particles and instead results in a stable colloidal suspension.[41] This approach enabled the temporal resolution of the growth and nucleation processes and the synthesis of several single-crystalline 2D COF colloids.[42] However, the underlying mechanism remains poorly understood, which stands as a barrier to the general application of this approach. Here, we use kinetic Monte Carlo (KMC) simulations to study the 2D COF nucleation and elongation rates as a function of initial monomer

concentration. Based on the simulation results, we are able to reach a *quantitative* understanding of the nucleation and growth rates, which we further validate via *in situ* X-ray scattering measurements. Overall our results allow us to rationalize why reducing the steady-state monomer concentration suppresses nucleation and favors crystallite growth, the strategy that has been successfully used in the fabrication of micron-sized 2D COF crystals.[42] This kinetic model will inspire other strategies to temporally resolve nucleation and growth. Similar control of initiation and propagation in linear polymerization has revolutionized precision polymer synthesis, and its further development in two-dimensional systems is key to fully realizing the potential of this longstanding missing topology in macromolecular science.

Results and Discussion

To probe the general dynamics of 2D COF polymerization, we focus on the boronate ester-linked COF-5, which is a frequently used model system in the study of 2D COFs.[35,38,41-45] COF-5 is formed from the condensation of 2,3,6,7,10,11-hexahydroxytriphenylene (HHTP) and 1,4-phenylenebis(boronic acid) (PBBA), as shown in **Scheme 1**. We have previously developed a kinetic Monte Carlo (KMC) model for 2D COF formation in solution, which makes use of a combination of experimentally and computationally derived parameters.[38] The rate parameters related to bond formation, bond breakage, and van der Waals interactions involved in the COF-5 growth have been parameterized in our previous work and found to reproduce very well the experimental production curves.[38] Here, in order to fully quantify the nucleation and growth rates, we carried out two sets of KMC simulations, based on modifications from our original KMC model.

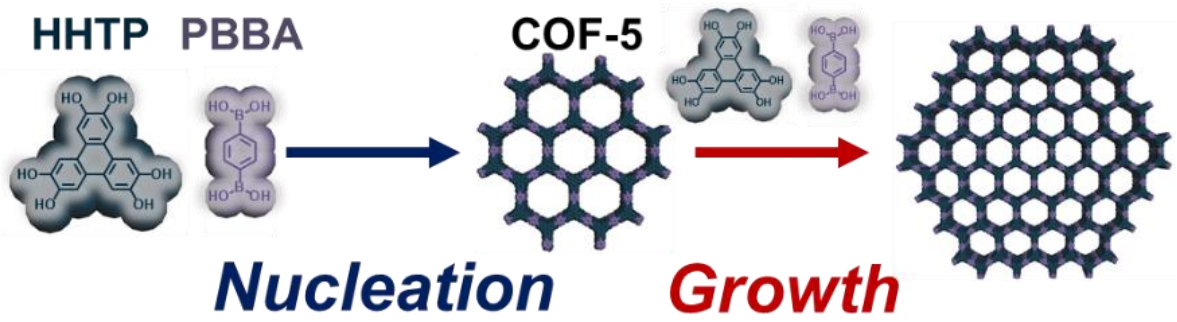

Scheme 1. The two-step growth process of micron-sized crystals obtained by slowly adding monomers to COF nanoparticle seeds[42].

The first set of simulations is designed to evaluate the nucleation rates. Here, the nuclei that have grown beyond a threshold size of 50 monomers are removed from consideration, thereby suppressing the impact of growth. The initial system contains 48,200 HHTP molecules and 72,300 PBBA molecules; the volume is varied in order to model different initial monomer concentrations. These amounts were chosen to minimize any finite-size effects (see **Figure S2** in the **Supporting Information**, **SI**) while still allowing for practical simulation times. The simulations are stopped when the nuclei that are generated correspond to 10% conversion of all monomers; in this way, the monomer concentrations do not vary significantly from their initial conditions. The nucleation rates are calculated through a linear fitting of nucleus production with time (additional computational details can be found in the **SI**). For each of the initial conditions, 20 simulations were run in order to reduce the statistical errors.

The second set of simulations focuses on the evaluation of growth rates by preventing additional nucleation after the appearance of the first nuclei. To model reliably large crystals, the system size is increased by a factor of ten so as to hold 482,000 HHTP molecules and 723,000 PBBA molecules. The simulations are completed when the crystal has grown to a size of 100,000

monomer units (which corresponds to less than 10% of the total number of monomers). The in-plane expansion/stacking rates are calculated by considering the evolution of the particle diameter/height *vs.* time. Similar to the first set of simulations, in order to obtain different initial monomer concentrations, the volume is varied while keeping the same number of monomers.

The results of the KMC simulations are shown in **Figure 1**. They establish the following fundamental relationships among the nucleation rate (J_{nuc}), the in-plane (lateral) expansion rate ($v_{in\text{-}plane}$), and the stacking (vertical expansion) rate ($v_{stacking}$), with respect to the monomer concentration ($C_{Monomer} = C_{HHTP} = 2/3\ C_{PBBA}$) –note that, for the sake of simplicity, we neglect the change in monomer concentration with respect to its initial value:

$$J_{nuc} = k_{nucleation} C_{monomer}^{2} \quad (1)$$

$$v_{in-plane} = k_{growth,in-plane} C_{monomer} \quad (2)$$

$$v_{stacking} = k_{growth,stacking} C_{monomer} \quad (3)$$

By considering a series of simulated monomer concentrations, we obtain that the $k_{nucleation}$, $k_{growth,in\text{-}plane}$, and $k_{growth,stacking}$ rate coefficients have values of 0.024 $L.mol^{-1}.s^{-1}$, 1,418 $nm.L.mol^{-1}.s^{-1}$ and 599 $nm.L.mol^{-1}.s^{-1}$, respectively.

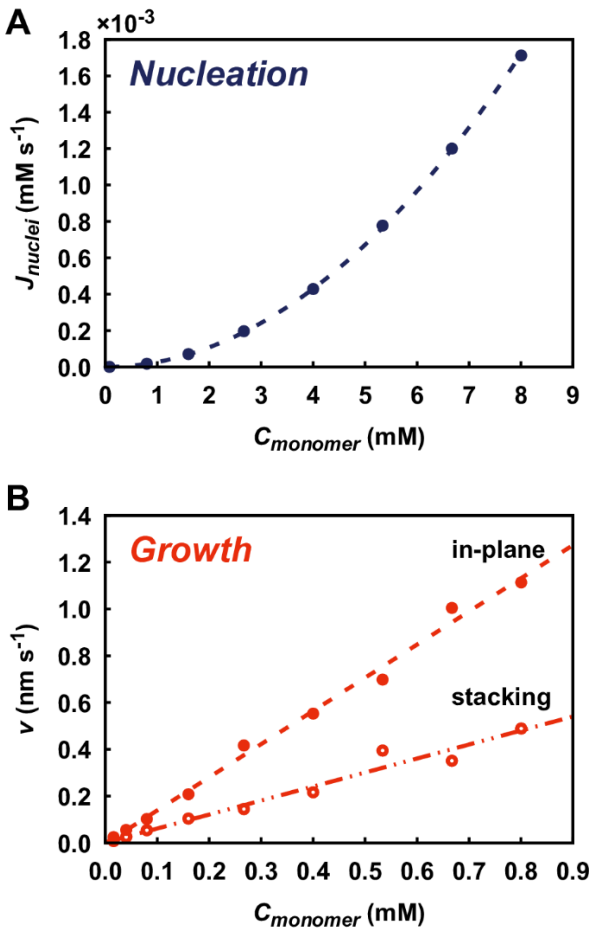

Figure 1. **A)** KMC-simulated nucleation rate as a function of monomer concentration. **B)** KMC-simulated in-plane and stacking growth rates as a function of monomer concentration.

Our earlier KMC simulations showed that nucleation involves bond formation and stacking between oligomers, which are both second-order in the reactants.[38] At steady state, the nucleation speed is expected to be governed by one of these two steps. Regardless of which step is the limiting one, a second-order dependence is preserved, as shown by **Eq. (1)**. The first-order dependence of growth on monomer concentration can be rationalized by considering that, while any growth is formally a second-order process, given that one reactant is fixed in the crystal, the overall dynamics become pseudo first-order.

Recently, Smith *et al.* reported an original methodology that allowed them to study COF-5 particles as homogenous colloidal suspensions.[41] These COF-5 nanoparticle solutions are much more suitable for mechanistic investigations than conventional agglomerated particles, since the heterogeneous processes of precipitation and aggregation are suppressed. Thus, we have measured the growth rates of the nanocrystalline colloidal suspensions in order to characterize in depth the mechanism of 2D COF growth.

To probe the rate dependence of COF-5 nucleation or growth, we turned to *in situ* Small/Medium/Wide-Angle X-ray Synchrotron Scattering (SAXS/MAXS/WAXS) measurements. The simultaneous collection of these data sets allowed us to monitor the size and crystallinity of the particles in tandem, as the reaction proceeded. To probe the nucleation and growth processes independently, it was necessary to choose conditions under which the processes were temporally resolved. This was achieved by selecting monomer concentrations under which one process dominated, as was seen for COF-5 in a recent report by Evans *et al*.[42] To probe the nucleation behavior of COF-5, we prepared solutions of HHTP and PBBA at concentrations of over 1 mM, which were recently demonstrated to favor nucleation. After heating these solutions to 70 °C, we continuously monitored the MAXS pattern during COF-5 nucleation (**Figure 2A**). The integrated intensity of the <100> Bragg feature (~0.24 $Å^{-1}$) as a function of time was extracted from these data (**Figure 2B**, inset). Finally, linear fits of signal intensity versus time were extracted to determine the rate of nucleation under these conditions. We observe a second-order relationship between the initial monomer concentration and the growth rate of the <100> signal intensity (**Figure 2B**). This observation is thus consistent with the results of the KMC simulations described above and supports a second-order dependence of COF nucleation on monomer concentration.

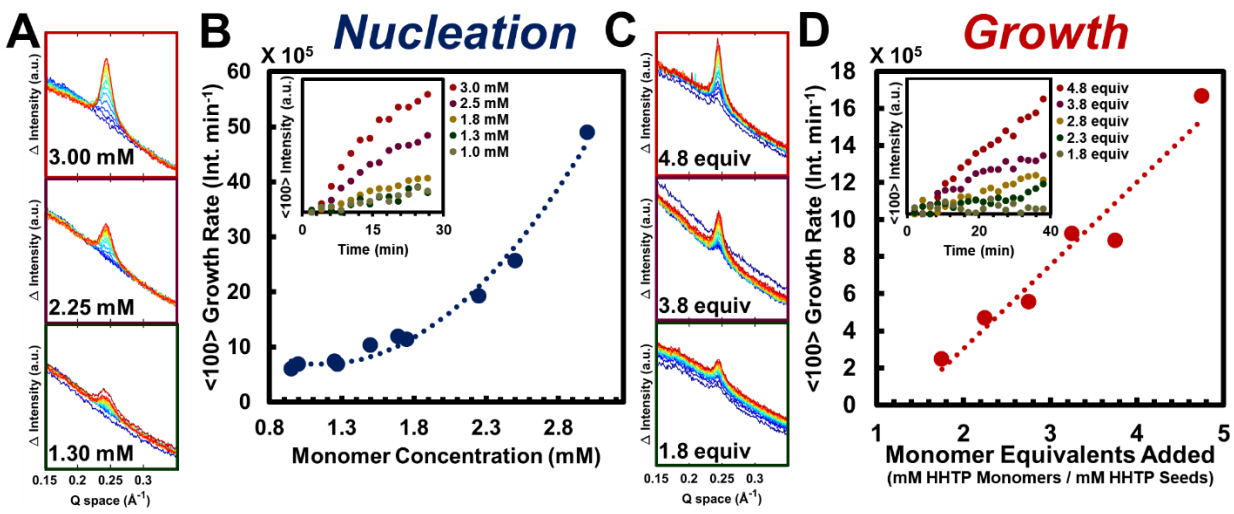

Figure 2. A) MAXS traces as a function of time for selected data of **B**. **B)** Rate of intensity of the <100> Bragg feature as a function of initial monomer concentration (inset: <100> intensity as a function of time for selected monomer concentrations). **C)** MAXS traces as a function of time for selected data of **D**. **D)** Rate of increase of intensity of the <100> Bragg feature as a function of monomer equivalents added (inset: <100> intensity as a function of time for selected equivalents added).

In order to probe the monomer dependence of growth, we sought to identify conditions under which nucleation would be suppressed, yet growth would occur at measurable rates. We first determined an upper concentration limit for growth experiments (0.7 mM) by allowing HHTP and PBBA to react in the absence of preexisting seed particles. No change in signal was observed, indicating that nucleation is suppressed at these time scales (**Figure S9**). It was also critical to identify concentrations of COF seeds that were observable while sufficiently dilute to allow for observable growth, which was ultimately optimized to an initial seed concentration. Mixtures of COF-5 seed particles at a constant particle density but variable free monomer equivalents (moles HHTP free monomer / moles of HHTP present in COF seeds) below this nucleation threshold were then prepared and heated to 70 °C (see **SI** for more details). Additionally, a sample was prepared

by diluting the COF-5 seeds in the absence of additional monomers. Once again, the MAXS pattern was monitored as a function of time (**Figure 2C**), with extracted <100> intensities (**Figure 2D** inset) and rate of this intensity growth (**Figure 2D**) being determined as described for the nucleation experiment. In this case, the <100> intensity growth rate is clearly linear with respect to the monomer equivalents (and therefore the initial monomer concentration) being added. As expected, under conditions where no additional monomers were added to the diluted COF seeds, the initial seed particles remained unchanged (**Figure S10**), which confirms that any enhancement in signal is not related to processes such as Ostwald ripening. Taken together, these results indicate that growth is a first-order process with respect to monomer concentration when the particle density of COF-5 seeds is held constant.

We stress that precise control of nucleation and growth rates is critical to fabricating high-quality 2D COF crystals. Based on the above results, it can be concluded that for COF-5 particles nucleation is an inherently higher-order process than growth. As we elaborate on in the following discussion, this difference in dynamics is the origin of the observation that nucleation and growth can be temporally resolved by controlling the monomer concentration, with nucleation being suppressed at lower monomer concentrations.[42,46]

We now turn to a discussion of the relative strengths of nucleation and growth rates. One way to compare these rates is through monomer consumption. The monomer consumption rates for nucleation ($\omega_{monomer,nuc}$) and growth ($\omega_{monomer,growth}$) of a crystal take on the following forms when assuming a cylindrical shape and a constant diameter-to-height ratio:

$$\omega_{monomer,nuc} = \mathrm{N}_{\mathrm{nuc}} J_{nuc} \propto C_{monomer}^{2} \qquad (4)$$

$$\omega_{monomer,growth} = \beta \frac{dV}{dt} \propto d^2 C_{monomer} \quad (5)$$

where N_{nuc} is the nucleus size, taken here as 50 monomer units; β, the number of monomer units per unit volume in the crystal; V, the crystal volume; t, the time; and d, the crystal diameter.

If we consider the monomer consumption rates of a colloidal system consisting of uniform microcrystals of diameter d, the steady-state nucleation and growth rates are sketched in **Figure 3A**. Therefore, the second- and first-order dependences of nucleation and growth rates on monomer concentration mean that there always exists a threshold concentration below which nucleation is slower than growth (**Figure 3A**). This analysis thus rationalizes the recent findings that nucleation is suppressed when adding monomers slowly to the colloidal solution.[42,46]

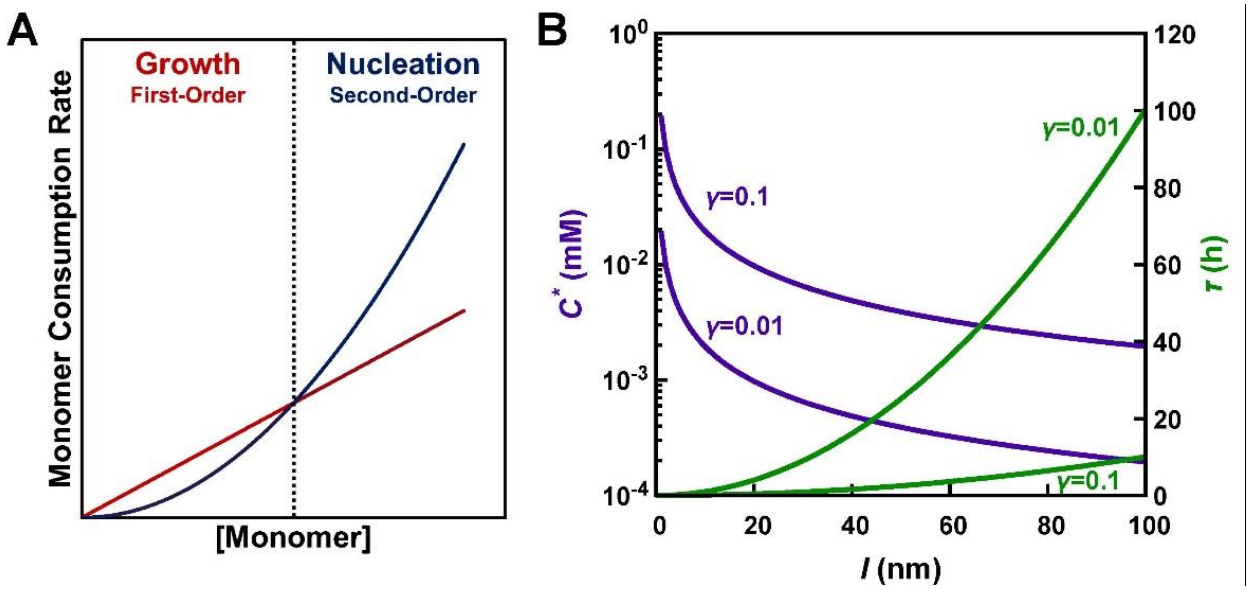

Figure 3. A) Comparison of the monomer consumption dynamics of nucleation and growth. **B)** Illustration of the critical monomer concentration and reaction time at different desired crystallite expansion (l). The value of $C_{nuc,0}$ is assumed to be 3.3×10^{-5} mM.

Understanding the relative rates of competing processes allows for guided experimental design of COF crystal growth by selecting a specific, steady-state monomer concentration. Higher monomer concentrations will speed the growth of existing colloids, yet complicates the suppression of the nucleation of new particles. Considering the interplay between nucleation and growth processes are always at play, it is challenging to completely eliminate nucleation. However, with the objective of suppressing nucleation, we define γ as the number of newly nucleated species divided by the initial seed crystals (it can be understood as a proportionality factor between the occurrence of new crystals with respect to the existing ones) during a growth process in which the diameter of the existing crystals is extended by l. There exists a critical monomer concentration (C^*) that represents the upper theoretical limit for a specific combination of γ and l. By this definition, the monomer concentration in the reaction needs to be lower than C^* to achieve the desired crystal expansion while suppressing nucleation. Monomer concentrations above C^* lead to more frequent nucleation (increased γ) and smaller average crystal sizes. We find that C^* depends on the initial nuclei concentration ($C_{nuc,0}$) and can be expressed as:

$$C^* = \frac{\gamma C_{nuc,0} k_{growth,in-plane}}{l k_{nucleation}} \tag{6}$$

The monomer consumption rate $\omega_{consump}$ (from both nucleation and growth) gives information about the monomer amount that should be added to maintain a constant monomer concentration at $C_{monomer}$. When assuming the crystals to be cylindrical and under the condition that $\gamma \ll 1$, we find that $\omega_{consump}$ is expressed as:

$$\omega_{consump} = \frac{3\pi k_{growth,in-plane} \beta C_{nuclei} C_{monomer}}{4\alpha} \left(k_{growth,in-plane} C_{monomer} t + d_0 \right)^2 + \mathrm{N}_{\mathrm{nuc}} k_{nucleation} C_{monomer}^2 \tag{7}$$

where α is the diameter-to-height ratio of the crystal and d_0, the initial diameter of the crystals. It emerges from **Eq. (7)** that $\omega_{consump}$ is not constant but instead increases quadratically with time.

For practical 2D COF growth, the reaction time is also an important factor to be considered. The use of too low a monomer concentration should be avoided as it results in undesirably slow growth. The shortest time for crystal growth is achieved when using $C_{monomer} = C^*$. In this case, the time required for the desired crystal expansion l is calculated to be:

$$\tau = \frac{l}{k_{growth,in-plane} C^*} = \frac{k_{nucleation} l^2}{k^2_{growth,in-plane} \gamma C_{nuclei,0}} \quad (8)$$

The quadratic dependence of time on desired growth coupled with the inverse dependence on γ means that growing ever larger crystals by slow monomer addition is likely to face practical challenges. Nevertheless, this analysis provides a theoretical reference for the monomer concentration to use during 2D COF fabrication, the amount of monomers to add, and the estimated time of crystal growth. This theoretical foundation is critical to the rational control over 2D COF synthetic conditions, and therefore temporal resolution of different microscale processes relevant to COF growth. Furthermore, the model we have developed for COF growth suggests that mechanisms other than direct condensation (*e.g.*, formal transimination [47] and monomer exchange reactions [48]) need to be explored to determine whether growth can be favored over nucleation, which could yield 2D COF single crystals under more practical time scales. In addition, we anticipate that combinations of strategies will likely be more effective than individual approaches.

Conclusions

The combination of kinetic Monte Carlo simulations and *in situ* X-ray scattering measurements has allowed us to develop a *quantitative* analysis of the nucleation and growth rates of 2D COFs, as represented by COF-5. The nucleation and growth processes have second-order and first-order dependences on monomer concentration, respectively. These different reaction orders explain why growth can be suppressed by controlling the speed of monomer addition. Based on this experimentally validated model, we were able to define a critical monomer concentration C^*, which provides insight into the optimal monomer concentration to use for 2D COF growth via slow addition of monomers to 2D COF colloidal seeds.

This understanding allows us to express several rules for the optimization of 2D COF synthesis. First, we find that C^* is proportional to the occurrence of new crystals with respect to the existing ones, while inversely proportional to the desired amount of expansion of the seed. Therefore, lower monomer concentrations should be selected when targeting fewer and larger crystallite domains. Secondly, C^* is linearly dependent on the number of nuclei in solution. This means that higher monomer concentrations may be used in solutions where the number of nuclei is also larger. Therefore, in solutions with more COF nanoparticles, the critical monomer concentration is increased as well as the rate of monomer consumption directed toward crystal growth. However, this growth will be shared among the larger number of crystallite seeds, making this strategy ineffective for increasing the average crystallite domain size more quickly.

The fundamental connection between C^* and the competition between nucleation and growth means that the reaction time has a quadratic dependence on the desired crystal expansion. While no theoretical upper limit exists in terms of a maximum COF size, the nonlinear dependence on

time suggests that growing large crystals can rapidly become impractical. For example, as illustrated by **Eq. (8),** growing 1-mm long crystals for a value of γ (the proportionality factor between the occurrence of new crystals with respect to the existing ones) equal to 0.01, can take over 1,000,000 years. Thus, growing millimeter-sized 2D COF crystals from solution using a direct-condensation, seeded-growth approach remains challenging. However, this limitation is associated with the specific strategy of limiting nucleation only by maintaining a low monomer concentration. Other methods to limit nucleation, such as chemically increasing the transesterification rate associated with COF formation, might provide access to high-quality COFs under different kinetic regimes. New synthetic strategies are called for to achieve these goals.

Finally, we note that 2D COF formation and growth can rely on different mechanisms. Here, we have used COF-5 as a representative example and the conclusions thus likely apply to the series of boronate ester-linked COFs. It will be of interest to determine whether the set of empirical equations developed here can be extended to other types of 2D COFs for which different growth mechanisms have been proposed. Such mechanistic investigations of chemically distinct systems are part of our ongoing collaborative efforts.

ASSOCIATED CONTENT

Supporting Information. Additional details on KMC simulations, the calculations of nucleation and growth rates and *in situ* XRD measurements. This material is available free of charge via the Internet at http://pubs.acs.org.

AUTHOR INFORMATION

Notes

The authors declare no competing financial interests.

ACKNOWLEDGMENTS

This work was supported by the Army Research Office, under the Multidisciplinary University Research Initiative (MURI) program, Award No. W911NF-15-1-0447, and under Grant No. W911NF-17-1-0339. A. M. E. (DGE-1324585), M.J.S. (DGE-1842165), and I.C. (DGE-1842165) are supported by the National Science Foundation Graduate Research Fellowship. I.C. is partially supported by the Ryan Fellowship and the International Institute for Nanotechnology. Parts of this work were performed at the DuPont-Northwestern-Dow Collaborative Access Team (DND-CAT) located at Sector 5 of the Advanced Photon Source (APS); DND-CAT is supported by Northwestern University, E.I. DuPont de Nemours & Co., and the Dow Chemical Company. This research used resources of the Advanced Photon Source and Center for Nanoscale Materials, both U.S. Department of Energy (DOE) Office of Science User Facilities operated for the DOE Office of Science by Argonne National Laboratory under Contract No. DE-AC0206CH11357.

REFERENCES

(1) Sakamoto, J.; van Heijst, J.; Lukin, O.; Schlüter, A. D., Two-Dimensional Polymers: Just a Dream of Synthetic Chemists?, *Angew. Chem., Int. Ed.* **2009**, *48*, 1030.
(2) Cote, A. P.; Benin, A. I.; Ockwig, N. W.; O'Keeffe, M.; Matzger, A. J.; Yaghi, O. M., Porous, Crystalline, Covalent Organic Frameworks, *Science* **2005**, *310*, 1166.
(3) Feng, X.; Ding, X. S.; Jiang, D. L., Covalent Organic Frameworks, *Chem. Soc. Rev.* **2012**, *41*, 6010.
(4) Wu, D. C.; Xu, F.; Sun, B.; Fu, R. W.; He, H. K.; Matyjaszewski, K., Design and Preparation of Porous Polymers, *Chem. Rev.* **2012**, *112*, 3959.

(5) Colson, J. W.; Dichtel, W. R., Rationally Synthesized Two-Dimensional Polymers, *Nature Chem.* **2013**, *5*, 453.
(6) Ding, S. Y.; Wang, W., Covalent Organic Frameworks (COFs): From Design to Applications, *Chem. Soc. Rev.* **2013**, *42*, 548.
(7) Bertrand, G. H. V.; Michaelis, V. K.; Ong, T.-C.; Griffin, R. G.; Dincă, M., Thiophene-Based Covalent Organic Frameworks, *Proc. Natl. Acad. Sci.* **2013**, *110*, 4923.
(8) Xu, H.; Gao, J.; Jiang, D., Stable, Crystalline, Porous, Covalent Organic Frameworks as a Platform for Chiral Organocatalysts, *Nature Chem.* **2015**, *7*, 905.
(9) Waller, P. J.; Gandara, F.; Yaghi, O. M., Chemistry of Covalent Organic Frameworks, *Acc. Chem. Res.* **2015**, *48*, 3053.
(10) Huang, N.; Wang, P.; Jiang, D., Covalent Organic Frameworks: A Materials Platform for Structural and Functional Designs, *Nat. Rev. Mater.* **2016**, *1*, 16068.
(11) Ascherl, L.; Sick, T.; Margraf, J. T.; Lapidus, S. H.; Calik, M.; Hettstedt, C.; Karaghiosoff, K.; Döblinger, M.; Clark, T.; Chapman, K. W.; Auras, F.; Bein, T., Molecular Docking Sites Designed for the Generation of Highly Crystalline Covalent Organic Frameworks, *Nature Chem.* **2016**, *8*, 310.
(12) Beuerle, F.; Gole, B., Covalent Organic Frameworks and Cage Compounds: Design and Applications of Polymeric and Discrete Organic Scaffolds, *Angew. Chem., Int. Ed.* **2018**, *57*, 4850.
(13) Lohse, M. S.; Bein, T., Covalent Organic Frameworks: Structures, Synthesis, and Applications, *Adv. Funct. Mater.* **2018**, *28*, 1705553.
(14) Bisbey, R. P.; Dichtel, W. R., Covalent organic frameworks as a platform for multidimensional polymerization, *Acs Central Science* **2017**, *3*, 533.
(15) DeBlase, C. R.; Silberstein, K. E.; Truong, T. T.; Abruna, H. D.; Dichtel, W. R., *β*-Ketoenamine-linked covalent organic frameworks capable of pseudocapacitive energy storage, *J. Am. Chem. Soc.* **2013**, *135*, 16821.
(16) Sun, B.; Zhu, C. H.; Liu, Y.; Wang, C.; Wan, L. J.; Wang, D., Oriented Covalent Organic Framework Film on Graphene for Robust Ambipolar Vertical Organic Field-Effect Transistor, *Chem. Mater.* **2017**, *29*, 4367.
(17) Miao, J.; Xu, Z.; Li, Q.; Bowman, A.; Zhang, S.; Hu, W.; Zhou, Z.; Wang, C., Vertically Stacked and Self-Encapsulated van der Waals Heterojunction Diodes Using Two-Dimensional Layered Semiconductors, *ACS Nano* **2017**, *11*, 10472.
(18) Dey, K.; Pal, M.; Rout, K. C.; Kunjattu H, S.; Das, A.; Mukherjee, R.; Kharul, U. K.; Banerjee, R., Selective Molecular Separation by Interfacially Crystallized Covalent Organic Framework Thin Films, *J. Am. Chem. Soc.* **2017**, *139*, 13083.
(19) Medina, D. D.; Sick, T.; Bein, T., Photoactive and Conducting Covalent Organic Frameworks, *Adv. Energy. Mater.* **2017**, *7*, 1700387.
(20) Xiang, Z. H.; Cao, D. P.; Dai, L. M., Well-defined two dimensional covalent organic polymers: rational design, controlled syntheses, and potential applications, *Polym. Chem.* **2015**, *6*, 1896.
(21) Pyles, D. A.; Crowe, J. W.; Baldwin, L. A.; McGrier, P. L., Synthesis of Benzobisoxazole-Linked Two-Dimensional Covalent Organic Frameworks and Their Carbon Dioxide Capture Properties, *ACS Macro Lett.* **2016**, *5*, 1055.
(22) Xu, Q.; Tao, S.; Jiang, Q.; Jiang, D., Ion Conduction in Polyelectrolyte Covalent Organic Frameworks, *J. Am. Chem. Soc.* **2018**, *140*, 7429.
(23) Zhao, F.; Liu, H.; Mathe, S.; Dong, A.; Zhang, J., Covalent Organic Frameworks: From Materials Design to Biomedical Application, *Nanomaterials* **2018**, *8*, 15.

(24) Zhao, W.; Xia, L.; Liu, X., Covalent organic frameworks (COFs): perspectives of industrialization, *CrystEngComm* **2018**, *20*, 1613.
(25) Wan, S.; Guo, J.; Kim, J.; Ihee, H.; Jiang, D., A Belt-Shaped, Blue Luminescent, and Semiconducting Covalent Organic Framework, *Angew. Chem., Int. Ed.* **2008**, *47*, 8826.
(26) Wan, S.; Gándara, F.; Asano, A.; Furukawa, H.; Saeki, A.; Dey, S. K.; Liao, L.; Ambrogio, M. W.; Botros, Y. Y.; Duan, X.; Seki, S.; Stoddart, J. F.; Yaghi, O. M., Covalent Organic Frameworks with High Charge Carrier Mobility, *Chem. Mater.* **2011**, *23*, 4094.
(27) Duhović, S.; Dincă, M., Synthesis and Electrical Properties of Covalent Organic Frameworks with Heavy Chalcogens, *Chem. Mater.* **2015**, *27*, 5487.
(28) Crowe, J. W.; Baldwin, L. A.; McGrier, P. L., Luminescent Covalent Organic Frameworks Containing a Homogeneous and Heterogeneous Distribution of Dehydrobenzoannulene Vertex Units, *J. Am. Chem. Soc.* **2016**, *138*, 10120.
(29) Jin, E.; Asada, M.; Xu, Q.; Dalapati, S.; Addicoat, M. A.; Brady, M. A.; Xu, H.; Nakamura, T.; Heine, T.; Chen, Q.; Jiang, D., Two-Dimensional sp^2 Carbon–Conjugated Covalent Organic Frameworks, *Science* **2017**, *357*, 673.
(30) Haldar, S.; Chakraborty, D.; Roy, B.; Banappanavar, G.; Rinku, K.; Mullangi, D.; Hazra, P.; Kabra, D.; Vaidhyanathan, R., Anthracene-Resorcinol Derived Covalent Organic Framework as Flexible White Light Emitter, *J. Am. Chem. Soc.* **2018**, *140*, 13367.
(31) Albacete, P.; Martínez, J. I.; Li, X.; López-Moreno, A.; Mena-Hernando, S. a.; Platero-Prats, A. E.; Montoro, C.; Loh, K. P.; Pérez, E. M.; Zamora, F., Layer-Stacking-Driven Fluorescence in a Two-Dimensional Imine-Linked Covalent Organic Framework, *J. Am. Chem. Soc.* **2018**, *140*, 12922.
(32) Wan, S.; Guo, J.; Kim, J.; Ihee, H.; Jiang, D. L., A Belt-Shaped, Blue Luminescent, and Semiconducting Covalent Organic Framework, *Angew. Chem., Int. Ed. Engl.* **2008**, *47*, 8826.
(33) Sick, T.; Hufnagel, A. G.; Kampmann, J.; Kondofersky, I.; Calik, M.; Rotter, J. M.; Evans, A.; Döblinger, M.; Herbert, S.; Peters, K.; Böhm, D.; Knochel, P.; Medina, D. D.; Fattakhova-Rohlfing, D.; Bein, T., Oriented Films of Conjugated 2D Covalent Organic Frameworks as Photocathodes for Water Splitting, *J. Am. Chem. Soc.* **2018**, *140*, 2085.
(34) Gonçalves, R. S. B.; de Oliveira, A. B. V.; Sindra, H. C.; Archanjo, B. S.; Mendoza, M. E.; Carneiro, L. S. A.; Buarque, C. D.; Esteves, P. M., Heterogeneous Catalysis by Covalent Organic Frameworks (COF): $Pd(OAc)_2$@COF-300 in Cross-Coupling Reactions, *ChemCatChem* **2016**, *8*, 743.
(35) Smith, B. J.; Dichtel, W. R., Mechanistic Studies of Two-Dimensional Covalent Organic Frameworks Rapidly Polymerized from Initially Homogenous Conditions, *J. Am. Chem. Soc.* **2014**, *136*, 8783.
(36) Smith, B. J.; Hwang, N.; Chavez, A. D.; Novotney, J. L.; Dichtel, W. R., Growth Rates and Water Stability of 2D Boronate Ester Covalent Organic Frameworks, *Chem. Commun.* **2015**, *51*, 7532.
(37) Medina, D. D.; Rotter, J. M.; Hu, Y.; Dogru, M.; Werner, V.; Auras, F.; Markiewicz, J. T.; Knochel, P.; Bein, T., Room Temperature Synthesis of Covalent–Organic Framework Films through Vapor-Assisted Conversion, *J. Am. Chem. Soc.* **2015**, *137*, 1016.
(38) Li, H. Y.; Chavez, A. D.; Li, H. F.; Li, H.; Dichtel, W. R.; Brédas, J.-L., Nucleation and Growth of Covalent Organic Frameworks from Solution: The Example of COF-5, *J. Am. Chem. Soc.* **2017**, *139*, 16310.
(39) De Yoreo, J. J.; Gilbert, P. U. P. A.; Sommerdijk, N. A. J. M.; Penn, R. L.; Whitelam, S.; Joester, D.; Zhang, H. Z.; Rimer, J. D.; Navrotsky, A.; Banfield, J. F.; Wallace, A. F.; Michel, F.

M.; Meldrum, F. C.; Colfen, H.; Dove, P. M., Crystallization by particle attachment in synthetic, biogenic, and geologic environments, *Science* **2015**, *349*, aaa6760.
(40) Sosso, G. C.; Chen, J.; Cox, S. J.; Fitzner, M.; Pedevilla, P.; Zen, A.; Michaelides, A., Crystal nucleation in liquids: Open questions and future challenges in molecular dynamics simulations, *Chem. Rev.* **2016**, *116*, 7078.
(41) Smith, B. J.; Parent, L. R.; Overholts, A. C.; Beaucage, P. A.; Bisbey, R. P.; Chavez, A. D.; Hwang, N.; Park, C.; Evans, A. M.; Gianneschi, N. C.; Dichtel, W. R., Colloidal Covalent Organic Frameworks, *ACS Central Science* **2017**, *3*, 58.
(42) Evans, A. M.; Parent, L. R.; Flanders, N. C.; Bisbey, R. P.; Vitaku, E.; Kirschner, M. S.; Schaller, R. D.; Chen, L. X.; Gianneschi, N. C.; Dichtel, W. R., Seeded Growth of Single-Crystal Two-Dimensional Covalent Organic Frameworks, *Science* **2018**, *361*, 52.
(43) Li, H. F.; Li, H. Y.; Dai, Q. Q.; Li, H.; Brédas, J. L., Hydrolytic Stability of Boronate Ester‐Linked Covalent Organic Frameworks, *Adv. Theory Simul.* **2018**, *1*, 1700015.
(44) Li, H. Y.; Brédas, J.-L., Large Out-of-Plane Deformations of Two-Dimensional Covalent Organic Framework (COF) Sheets, *J. Phys. Chem. Lett.* **2018**, *9*, 4215.
(45) Li, H. Y.; Brédas, J.-L., Nanoscrolls Formed from Two-Dimensional Covalent Organic Frameworks, *Chem. Mater.* **2019**, *31*, 3265.
(46) Li, Rebecca L.; Flanders, N. C.; Evans, A. M.; Ji, W.; Castano, I.; Chen, L. X.; Gianneschi, N. C.; Dichtel, W. R., Controlled growth of imine-linked two-dimensional covalent organic framework nanoparticles, *Chem. Sci.* **2019**, *10*, 3796.
(47) Vitaku, E.; Dichtel, W. R., Synthesis of 2D Imine-Linked Covalent Organic Frameworks through Formal Transimination Reactions, *J. Am. Chem. Soc.* **2017**.
(48) Daugherty, M. C.; Vitaku, E.; Li, R. L.; Evans, A. M.; Chavez, A. D.; Dichtel, W. R., Improved synthesis of β-ketoenamine-linked covalent organic frameworks via monomer exchange reactions, *Chem. Commun.* **2019**, *55*, 2680.